Journal of Earth Science, *Vol. xx*, *No. x. xxx–xxx*, *online 2019* *ISSN 1674-487X*
Printed in China
https://doi.org/10.1007/s12583-019-1212-2

Geomorphologic Characteristics of Polygonal Features on Chloride-Bearing Deposits on Mars: Implications for Martian Hydrology and Astrobiology

Binlong Ye[1], **Jun Huang***[1], **Joseph Michalski**[2], **Long Xiao**[1]
1. *Planetary Science Institute*, *School of Earth Sciences*, *China University of Geosciences*, *Wuhan* 430074, *China*
2. *Department of Earth Sciences and Laboratory for Space Research*, *University of Hong Kong*, *Hong Kong* 999077, *China*
Binlong Ye: https://orcid.org/0000-0002-7177-8982; Jun Huang: https://orcid.org/0000-0003-0168-6633

ABSTRACT: Over 600 chloride-bearing deposits (chlorides) have been identified on the southern highlands of Mars. These chlorides have critical implications for hydrology and astrobiology: they are indicators of an evaporating super saturated solution, and they could have provided habitat environments for halophilic microorganisms and preserved organic matter. One of the prominent geomorphology characteristics of these chloride-bearing regions is the polygonal features within them. The origin of these polygonal features is still in debate. In this study, we have surveyed 153 locations of chlorides using 441 high resolution imaging science experiment (HiRISE) images to characterize the geomorphology of polygonal features. We identified 3 types of polygonal features of distinct geomorphologic characteristics: fractures, raised ridges, and transitional polygons between fractures and raised ridges. We evaluate previously proposed hypotheses of the formation of the polygonal features, and suggest that the 3 types of polygonal features are indicators of different stages of salt crust formation. Salt crust is usually formed through multiple groundwater activities, and it often occurs in playa environment on Earth. The unique hydrological and astrobiological implications of the chlorides with polygonal features make these deposits of high priority for future landed on and/or sample return exploration missions of Mars.
KEY WORDS: chlorides, polygonal feature, playa, hydrology, astrobiology, Mars.

0 INTRODUCTION

Over 600 chloride-bearing deposits (chlorides) have been identified (Osterloo et al., 2010, 2008) on the southern highlands of Mars. The chlorides exhibit a negative spectral slope lacking diagnostic emission features over mid-infrared (MIR) wavelengths in thermal emission spectrometer (TES) (Christensen et al., 2001) and Thermal Emission Imaging System (THEMIS) (Christensen et al., 2004) spectral data. The visible/near-infrared (VNIR) spectrum acquired by compact reconnaissance imaging spectral for Mars (CRISM) (Murchie et al., 2009) of the chlorides shows a distinctive spectrally featureless red slope, and it has high reflectance values near 3.0 μm in ratioed spectra, indicating dehydration in chlorides relative to typical silicate-bearing materials (Fig. 1) (Ruesch et al., 2012; Jensen and Glotch, 2011; Osterloo et al., 2010, 2008; Murchie et al., 2009). The chlorides occur on the Middle Noachian to the Early Hesperian terrains of the southern highlands (Osterloo et al., 2010), and most of them appear small, spatially isolated patches in local shallow close basins (Fig. 2). They also occur within inverted sinuous channels (Fig. 2a), impact craters (Fig. 2b) and inter-crater plains (Fig. 2c) (Osterloo et al., 2010, 2008).

Several hypotheses have been proposed to explain the geologic setting of chlorides, such as hydrothermal brine caused by impact or volcanic activity (Osterloo et al., 2010), efflorescence generated through atmospheric interactions or fumarolic activity (Osterloo et al., 2010), evaporation from ponds supplied by surface runoff (Hynek et al., 2015; Osterloo et al., 2008) or groundwater upwelling (Ruesch et al., 2012) or combination of both (Glotch et al., 2016).

One of the most prominent geomorphological features within the chlorides is polygonal features of different sizes, which were interpreted as desiccation cracks (Osterloo et al., 2010, 2008). El-Maarry et al. (2013) analyzed polygonal features within ~80 locations of chlorides using ~90 HiRISE images and available CRISM data, along with comparative studies of terrestrial dried lakes and playas, and they found that the polygonal features occurred within the chlorides are due to the existence of Fe/Mg smectites (El-Maarry et al., 2013). However, phyllosilicate bearing materials are not commonly identified with chlorides, except in few locations, e.g., northwestern Terra Sirenum (Ruesch et al., 2012; Glotch et al., 2010), and west of Knobel crater (Huang et al., 2018). Therefore, it is very challenging to explain the existence of polygonal features owing to the mixing of Fe/Mg smectites, although El-Maarry et al. (2013) argued that the absence of smectites spectral signatures might be due to dust cover or relatively high chloride concentration. The formation mechanism of the polygonal features is critical to understand the origin of chlorides, which has important hydrology and astrobiology implications.

*Corresponding author: junhuang@cug.edu.cn

Manuscript received May 10, 2018.
Manuscript accepted September 11, 2018.

Ye, B. L., Huang, J., Michalski, J., et al., 2019. Geomorphologic Characteristics of Polygonal Features on Chloride-Bearing Deposits on Mars: Implications for Martian Hydrology and Astrobiology. *Journal of Earth Science*, xx(x): xxx–xxx. https://doi.org/10.1007/s12583-019-1212-2. http://en.earth-science.net

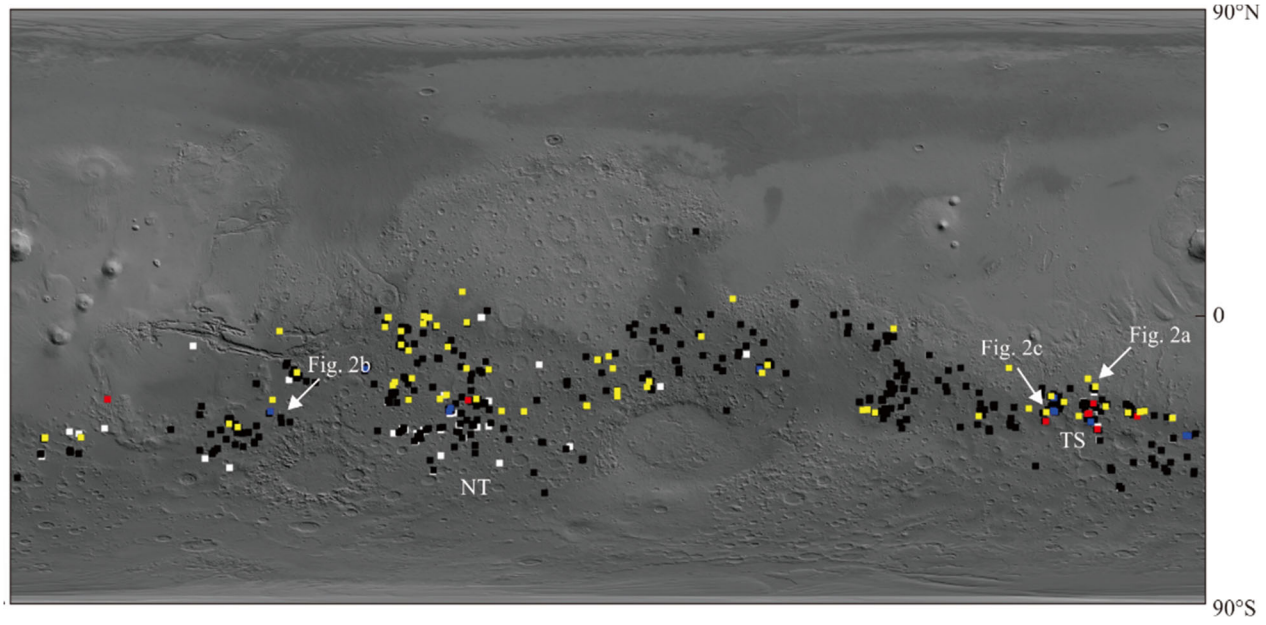

Figure 1. Global distribution of 642 chlorides on Mars (Osterloo et al., 2010). The dots represent the locations of chlorides on Mars. Yellow dots indicate the locations of fracture polygon (67 regions). Blue dots represent the locations of transitional polygon (11 regions). Red dots show the locations of raised ridge polygon (17 regions). White dots exhibit the region where no crack has been observed (65 regions). Black dots show the areas where no HiRISE image (490 regions). The context map is Mars orbiter laser altimeter (MOLA) shaded relief data overlain by TES Lambert albedo. NT and TS stand for Noachis Terra and Terra Sirenum, respectively.

In this study, we conducted a comprehensive global survey to polygonal features on 153 sites of chlorides using 441 HiRISE images. We characterized meter-scale polygonal features and grouped them into three types based on their geomorphologic characteristics. Then, we evaluated previously proposed hypotheses of the formation mechanism of the polygonal features, and proposed that the three types of polygonal features are indicators of different stages of salt crust formation. These chlorides with polygonal features have hydrology and astrobiology implications, which make them high priority in future landed on and/or sample return mission.

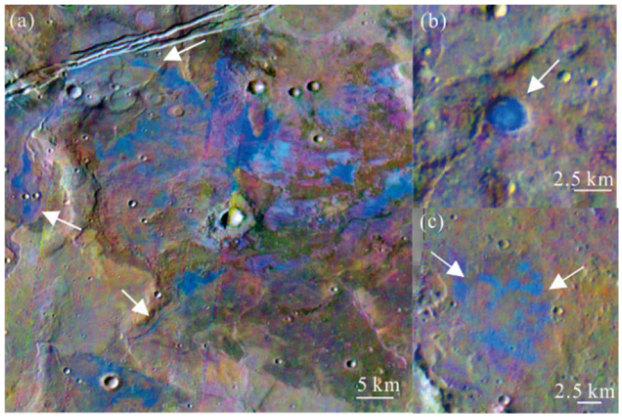

Figure 2. THEMIS TIR decorrelation stretch (DCS) radiance images. Red, green and blue channels are assigned as bands 8, 7 and 5, respectively. The chlorides are identified in the blue tone areas. (a) A relatively large region of chlorides, the white arrows point to sinuous channels filled with chlorides (centered at ~-32.85°S, ~204.97°E); (b) chlorides occur in a small carter (centered at ~33.44°S, ~306.67°E); (c) small patches of chlorides occur in the basin floor (centered at ~31.1°S, ~180.2 °E).

1 METHODS

We use THEMIS data as a guide for chlorides identification. The THEMIS instrument is a multiband visible-thermal infrared (TIR) camera with 5 visible/near infrared bands (Christensen et al., 2004) onboard Mars Odyssey spacecraft. The TIR data is sampled at 100 m/pixel spatial resolution with nine bands in wavelength from ~6.8 to 14.9 μm, providing information of temperatures, compositions and thermophysical properties of the surface materials (Christensen et al., 2004). THEMIS products were processed using standard THEMIS IR processing procedures to correct instrument and atmospheric effects according to Bandfield (2004). Calibrated THEMIS daytime TIR data were processed to produce decorrelation stretch (DCS) products, which could qualitatively enhance compositional variation (Edwards et al., 2011; Gillespie et al., 1986). The chlorides have a special blue tone color in DCS composed of band 8 (11.75 μm), band 7 (10.99 μm) and band 5 (9.30 μm) (Fig. 3) (Osterloo et al., 2008). The distinct tone is due to spectral slope in homogeneously low in the wavelength of 6.78 to 14.88 μm of THEMIS day IR data.

We use context camera (CTX) images (Malin et al., 2007) to provide regional context for HiRISE images. The CTX instrument is onboard Mars reconnaissance orbiter (MRO), and it acquires panchromatic images with spatial sampling of ~6 m/pixel.

Detail geomorphologic characteristics were analyzed using HiRISE images. HiRISE is a visible imaging system onboard the MRO, providing unprecedented spatial resolution images of ~0.25 m/pixel resolution (McEwen et al., 2007). HiRISE is equipped red-filter channels for panchromatic images and NIR and blue-green filters for color images (McEwen et al., 2007). The central wavelength of red filter is 694 nm, the blue-green filter is 536 nm and the NIR wavelength is 874 nm (McEwen et

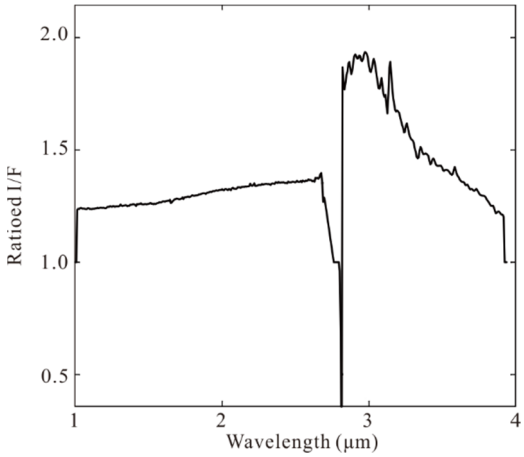

Figure 3. Visible/near-infrared ratioed spectrum of chlorides from CRISM data FRT0000B0001. It shows a distinctive spectrally featureless red slope with high reflectance values near 3.0 μm indicating dehydration in chlorides relative to typical silicate-bearing materials.

al., 2007). The color images of HiRISE are powerful to identify compositional and roughness variations at sub-meter scales (Wray et al., 2009; Herkenhoff et al., 2007; Okubo and McEwen, 2007). We used stereo pairs of HiRISE (ESP_036509_1485 and ESP_052768_1485) images to produce digital terrain models (DTM) with Ames Stereo Pipeline (Shean et al., 2016). The HiRISE DTM could allow us to conduct detailed topographic research (Kirk et al., 2008).

2 RESULTS

Osterloo et al. (2010) have built a global database of chlorides on Mars, which includes 641 distinct sites. We found 441 HiRISE images covered 153 sites from Osterloo et al. (2010) database. After examining these 153 sites of chlorides using overall HiRISE, we identified three types of polygonal features, including fractures, raised ridges, and transitional polygons. We also recorded the detailed geometric characteristics of the polygon features.

The fracture polygon is identified by network fracture within polygons (Fig. 4). We have identified 67 locations of chlorides containing fracture polygons (Fig. 1). Most of them concentrate between 0°S to 30°S across the southern highlands. Nearly all polygonal features in Noachian Terra fall in this type. The shape of the polygon fractures usually occurs in quadrangle, and the rims of the polygons are generally straight. The sizes of the polygonal fractures range from ~2 to ~50 m, while the width of trough varies from ~0.2 to ~2 m. The region of cracks looks relatively dark comparing to the adjacent terrain, indicating synchronous and/or post-formation infillings (Fig. 4).

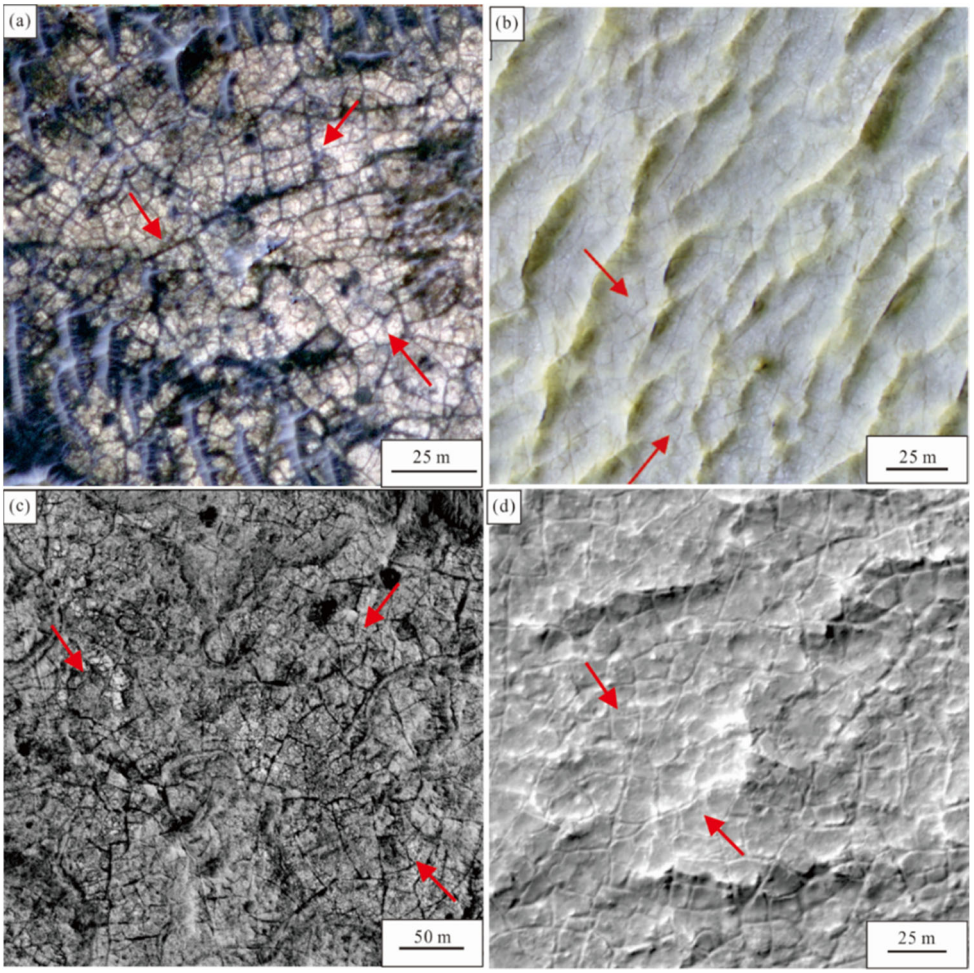

Figure 4. Red arrows point to fracture polygonal features of chloride-bearing depositions on Mars. HiRISE Image ID: (a) ESP_16288_1745_COLOR; (b) ESP_049427_1600_COLOR; (c) ESP_012741_1750_RED; (d) ESP_034732_1600_RED.

The raised ridge polygonal feature is characterized by prominent raised ridges (Fig. 5). We identified 17 locations of raised ridge polygonal features. They appear to cluster in Terra Sirenum (Fig. 1). The shapes of the raised ridge polygon are quadrangle and hexagon. Their sizes range from ~10 to ~15 m, and the rims of the polygons are generally straight. The regions of the raised ridges are usually relatively brighter than their interiors. However, the areas of rims show relatively uniformed tone in HiRISE color images. The widths of rims range from ~0.5 to ~2 m. Instead, we use incidence angle of the scene and number of the pixels of the shadow region of the rims to estimate their heights. The shadow is usually ~1–2 pixel, and it's hard to provide the height of ridge accurately, but it could be the upper limit. The heights are generally less than ~1 m (Fig. 6). We also use the HiRISE DTM to conduct detailed study and we found little topography relief (Fig. 7).

The transitional type polygonal feature is identified by cracks occurring in the raised ridges of the polygons (Fig. 8). This type polygon is an intermedia form between fracture and raised ridge. We have identified a type of transitional polygons in 11 sites of chlorides (Fig. 1). The sizes of the transitional polygons range from ~5 to ~15 m.

We have not identified polygonal features in the remaining 65 locations (Fig. 1). These sites lie in the east of Argyre Basin (south of Noachis Terra). The surface of the chlorides is generally ridged, relatively bright and boulder-less than the surrounding terrain.

There are several possibilities to explain that we did not observe polygons in some of the chlorides-bearing region: (1) Those could be formed in a different mechanism, like hydrothermal brine caused by impact or volcanic activity (Osterloo et al., 2010), efflorescence generated through atmospheric interactions or fumarolic activity (Osterloo et al., 2010); (2) the polygons have been wiped out by subsequent geological process, like seasonally deliquesce (Davila et al., 2010), which may change the geomorphology of chlorides.

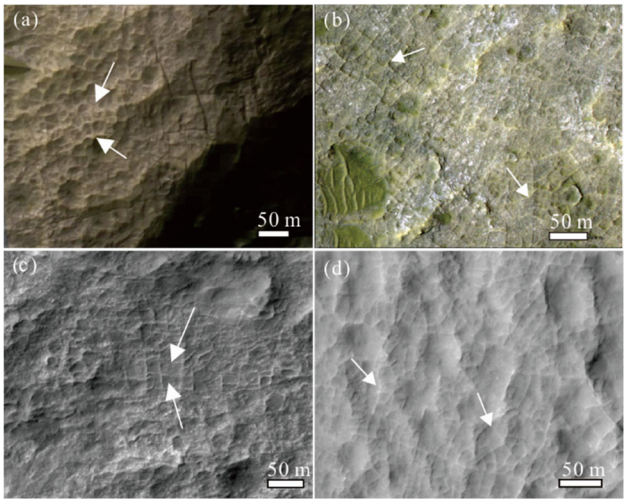

Figure 5. White arrows point to the raised ridge polygonal features of chlorides. HiRISE image ID: (a) ESP_044165_1610_COLOR; (b) ESP_047343_1610_COLOR; (c) ESP_010387_1485_RED; (d) ESP_011547_1475_RED.

3 DISCUSSION

3.1 Formation Mechanism of the Raised Ridge Polygonal Features

The polygonal fracture is initially interpreted as desiccation origin, which is a common phenomenon in dried lakes, and dried farmlands on Earth. However, desiccation alone is difficult to interpret the raised ridge polygonal features of chlorides on Mars based on the observations described in previous section. El-Maarry et al. (2013) proposed that the polygonal features are likely formed by mixing of Fe/Mg smectites, but the spectral evidence of coexisting of Fe/Mg smectites and chloride is very limited (Huang et al., 2018; Ruesch et al., 2012; Glotch et al., 2010).

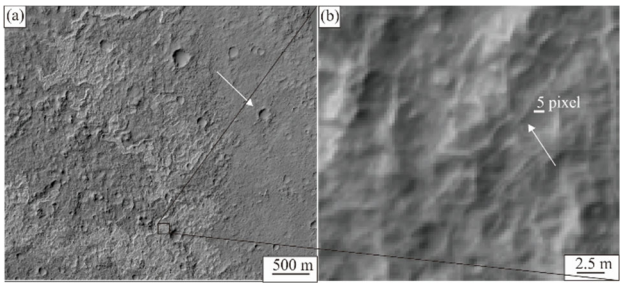

Figure 6. Demonstration of shadow measurement technique on raised ridge polygonal features of chlorides. (a) HiRISE image of the raised ridge polygonal features, the white rectangle indicates the location of (b), the white arrow indicates the incident direction of the sunlight, (b) the white arrow points to the shadow, the maximum length of the shadow is 3 pixel, about 1.5 m, the solar incident angle is 73°. Using the trigonometric function to calculate the maximum height of raised ridge, the height is ~0.45 m. HiRISE image ID: ESP_036509_1485_RED.

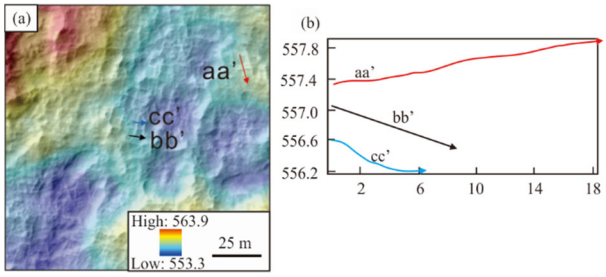

Figure 7. (a) HiRISE ESP_036509_1485 overly on HiRISE DEM, the arrow means the end of the profile line; (b) the profile shows little topography relief.

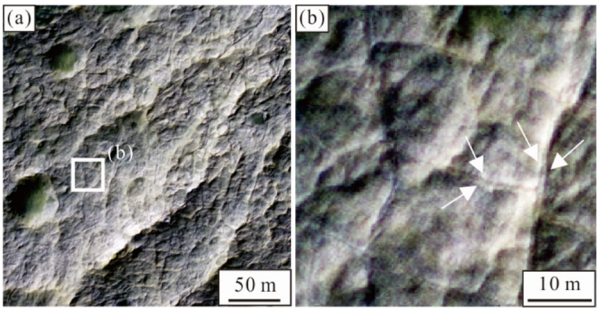

Figure 8. (a) Transitional polygons, the black rectangle represents the location of b; (b) the white arrows point to the ridges of transitional polygonal features. HiRISE image ID: PSP_008720_1610_COLOR.

Many raised ridge polygons, also known as polygonal ridge networks, boxwork or reticulate ridges have been observed in extensive locations and geological contexts across Mars (Stein et al., 2018; Kerber et al., 2017; Ebinger and Mustard, 2015; Saper and Mustard, 2013; Thomason, 2011; Mangold et al., 2007; Head and Mustard, 2006). The possible formation mechanisms of the polygonal ridge networks (Kerber et al., 2017) include: (1) intrusions by volcanic dikes under an unusual stress field, (2) intrusion by volcanic dikes along pre-existing polygonal faults, (3) breccia dikes formed during impact, (4) deposition of minerals along pre-existing fractures (veins), (5) chemical alteration of pre-existing fracture planes by circulating groundwater, (6) sedimentary infilling of pre-existing open cracks, and (7) induration of a pre-existing polygonal dune or transverse aeolian ridge (TAR) network. Intrusion by volcanic dikes under an unusual stress field, intrusion by volcanic dikes along pre-existing polygonal faults, chemical alteration of pre-existing fracture planes by circulating groundwater and sedimentary infilling of pre-existing open cracks are unlikely responsible for the raised ridge in the chlorides. These locations are close to valley networks (Hynek et al., 2010) and valley-fed basins (Fassett and Head, 2008), not close to the region hosting minerals related to volcanic origin minerals (e.g., Olivine, Pyroxene; Ruesch et al., 2012; Osterloo et al., 2010). Also, the regions of the raised ridges are relatively bright than their surrounding materials, but the tone of the raised ridges and interiors of the spolygons is similar in color HiRISE images, which indicates the raised ridges are formed with the polygons and suggests similar composition. As well, the THEMIS DCS 875 images show the homogeneous blue tone of chlorides on Mars. The thermal inertia of chlorides derived from THEMIS generally display at least ~400 $Jm^{-2}K^{-1}s^{-1/2}$ and up to 509 $Jm^{-2}K^{-1}s^{-1/2}$ and have relatively homogenous thermophysical properties (Osterloo et al., 2010), which also suggest similar composition between the raised ridge and its interior. If the volcanic dike filled in the polygonal cracks, it should have heterogeneous THEMIS DCS 875 and thermal inertia. The breccia dikes formed during a meteorite impact is used to explain the raised ridges, up to several kilometers in size in Nili Fossae region (Fig. 9) (Head and Mustard, 2006). The magnitude of the polygonal features of the impact breccia dikes is much larger than the meter-scale polygonal features of chlorides we observed in this study. It indicates the raised ridges are formed with the polygons, which rules out the hypotheses of induration of a pre-existing polygonal dune or transverse aeolian ridge (TAR) network. In addition, the transverse aeolian ridges (TARs) are found primarily at the bottom of crater floors, and they usually degrade into linear transverse ridges when topography changes (Kerber et al., 2017).

Another potential hypothesis of the origin of the raised ridges polygonal features is thermal contraction (Mellon et al., 2008; Mangold, 2005; Mutch et al., 1976). Thermal contraction polygons have been widely explored and characterized by orbiting and landing missions for more than 30 years on Mars. One of the 7 previously proposed thermal contraction polygons (Levy et al., 2009a) is similar in size and morphology to the raise ridges we observed. These polygons have central depressions, raised rims, and near-orthogonal and near-hexagonal shapes (Fig. 10). The sizes are ~20 m in the southern hemisphere, while ~11.3 m in the northern hemisphere (Levy et al., 2009a). They are mainly identified in latitude dependent mantle deposits (Levy et al., 2009b) of Utopia Planitia (Soare et al., 2008), circum-Hellas and Argyre terrains (Zanetti et al., 2010; Morgenstern et al., 2007).

However, our observations are inconsistent with the formation mechanism of thermal contraction. The latitudes, albedos and surface ages of the chlorides in study are different from those of regions with thermal contraction origin. Polygonal features interpreted as thermal contraction origin are present primarily in regions of latitude larger than 30°, because ground ice is the major factor controlling the formation mechanisms, while previous, models predict that the ground ice is not stable in

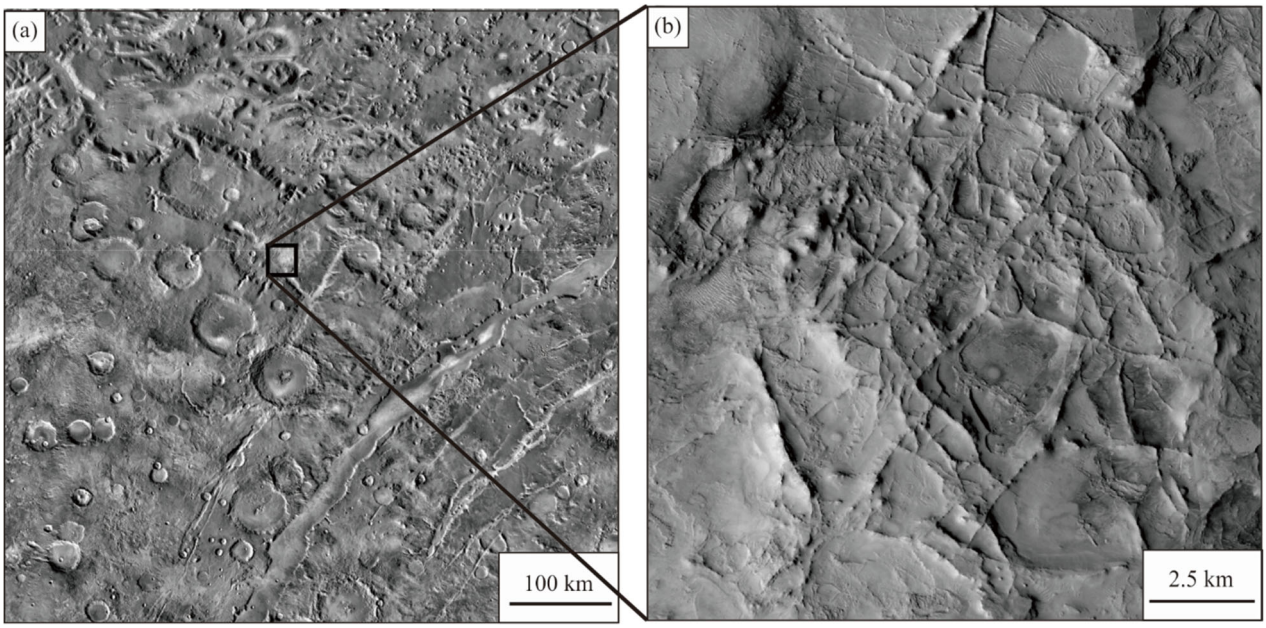

Figure 9. (a) THEMIS IR Day mosaic images of Nili Fossae region; (b) kilometer size raised ridge polygon in Nili Fossae region. HiRISE image ESP_018065_1975_RED.

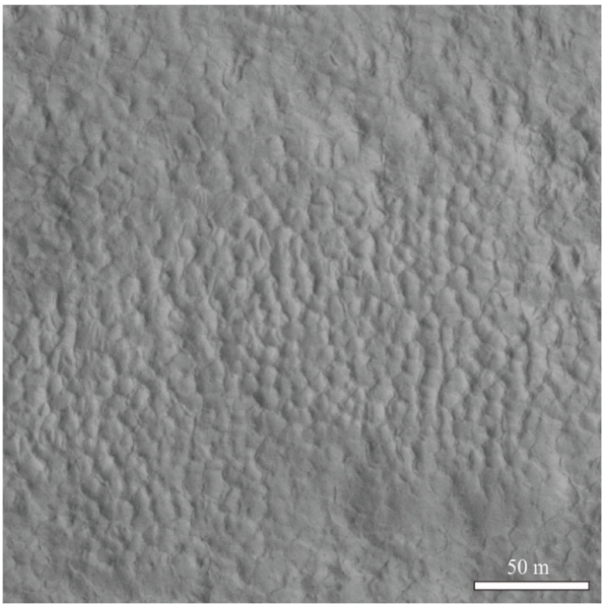

Figure 10. Polygonal features formed through thermal contraction process. HiRISE ESP_011523_2235_RED (centered at ~42.95°N, 115.67°E).

equatorial region (0°~30°) (Mellon et al., 2004; Mellon and Jakosky, 1995). The albedo of thermal contraction polygons is moderate to low, while the polygonal features of chlorides are relatively high in albedo (Levy et al., 2009a). The thermal contraction origin polygons occur within latitude dependent mantle deposits, which is Amazonian age. However, the chlorides are of the Middle Noachian to the Early Hesperian ages, which is inconsistent with the much younger age of thermal contraction hypothesis. Salt crust on Earth could be a possible counterpart of the raised ridge polygonal features we observed on Mars. Salt crust is a common landform in halide playa on Earth, such as playas in Qaidam Basin, NW China (Anglés and Li, 2017; Xiao et al., 2017; Yi et al., 2017; Zeng and Xiang, 2017; Wang et al., 2013) (Fig. 11), Iran (Krinsley, 1970) and Oman (Thomas, 2011). The chlorides on Mars is similar in geologic context of playa on Earth. In terrestrial playa, salt crust located in a relatively depressed region, while on Mars, most of the chlorides appear small, spatially isolated patches in local shallow close basins (Osterloo et al., 2010, 2008). The slope map of raised ridge polygonal features of chlorides on Mars shows the slope of this regions is generally smaller than 5° (Fig. 12), which is consistent with flat or gently declined background landform in terrestrial playa. The geomorphological features are striking resemble. The polygonal features on Mars are asymmetric, which also is similar on the playa of Earth. Generally, the height of the ridges in terrestrial playa can reach up to ~50 cm. We used the shadow measurement technique and HiRISE DTM to constrain the height of raised ridge of chlorides on Mars. The heights are generally less than ~1 m, which is close to the height of the raised ridges in the terrestrial salt crust. The formation process of salt crust on Earth has been studied in detail: At first, intense evaporation and annually capillary upflow lead to the precipitation of salts (Thomas, 2011; Christiansen, 1963) (Figs. 13b, 13c). Then the growth of the salt crystals and increasing summer temperature generate compressional stresses to form the polygonal features (Christiansen, 1963). Then, with the rehydration of salts through limited episodic brine and re-precipitation due to the intensive seasonal evaporation, the fractures enlarge and successive crystal growth trigger and expand to form the raised ridges (Anglés and Li, 2017; Xiao et al., 2017; Thomas, 2011) (Figs. 13h, 13i).

The different types polygonal features we observed on Mars: polygonal fractures (Fig. 13a), intermedia polygonal features (Fig. 13d), and raised ridges polygons (Fig. 13g), are also similar with different stages of salt crust formation in terrestrial playa, respectively (Figs. 13b, 13e, 13h). The average THEMIS thermal inertia is 295±45 $Jm^{-2}K^{-1}s^{-1/2}$ (Osterloo et al., 2010), suggesting the materials have the grain size that is generally greater than ~900 μm and/or consistent with indurated materials (Putzig et al., 2005), which also supports the playa setting. So, we propose the raised ridge of chlorides on Mars is salt crust and the similar process may shape the raise ridge polygonal features of the chlorides on Mars.

In addition, groundwater activity plays a key role in salt crust formation process described above. If the raised ridges form through the similar process, it would preserve other pieces of evidence of groundwater activity. We found raised ridge polygons mostly concentrate in the Terra Sirenum region (Fig. 1). Previous study proposed that the Terra Sirenum region experienced intense groundwater active predicted by hydrological model (Andrews-Hanna and Lewis, 2011). Detailed regional geology study of Cross Crater, Dejnev Crater and Columbus Crater also reveal strong groundwater activities and evaporation mineral formation (Ehlmann et al., 2016; Wray et al., 2011). Both model prediction and geology evidence are consistent with the salt crust hypothesis.

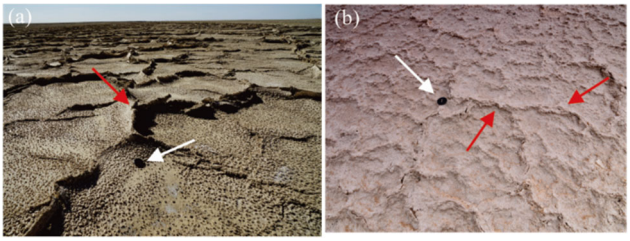

Figure 11. Salt crust in Qaidam Basin, NW China. The white arrow points to the lens cap. The red arrow points to the raised rim feature on salt crust, the lens cap is ~20 cm.

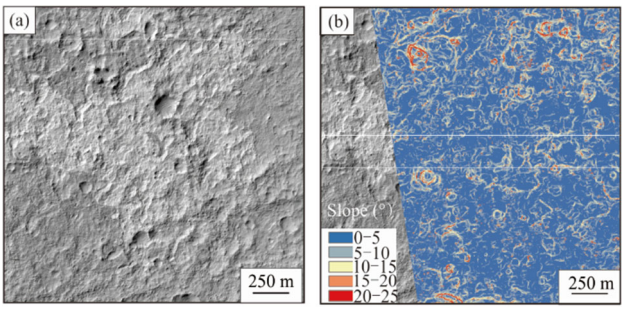

Figure 12. (a) The raised ridge polygonal features. HiRISE ID: ESP_036509_1485. The white line indicates the extent of chlorides, (b) slope map of the raised ridge polygon region from HiRISE DTM derived from stereo pairs ESP_036509_1485 and ESP_052768_1485.

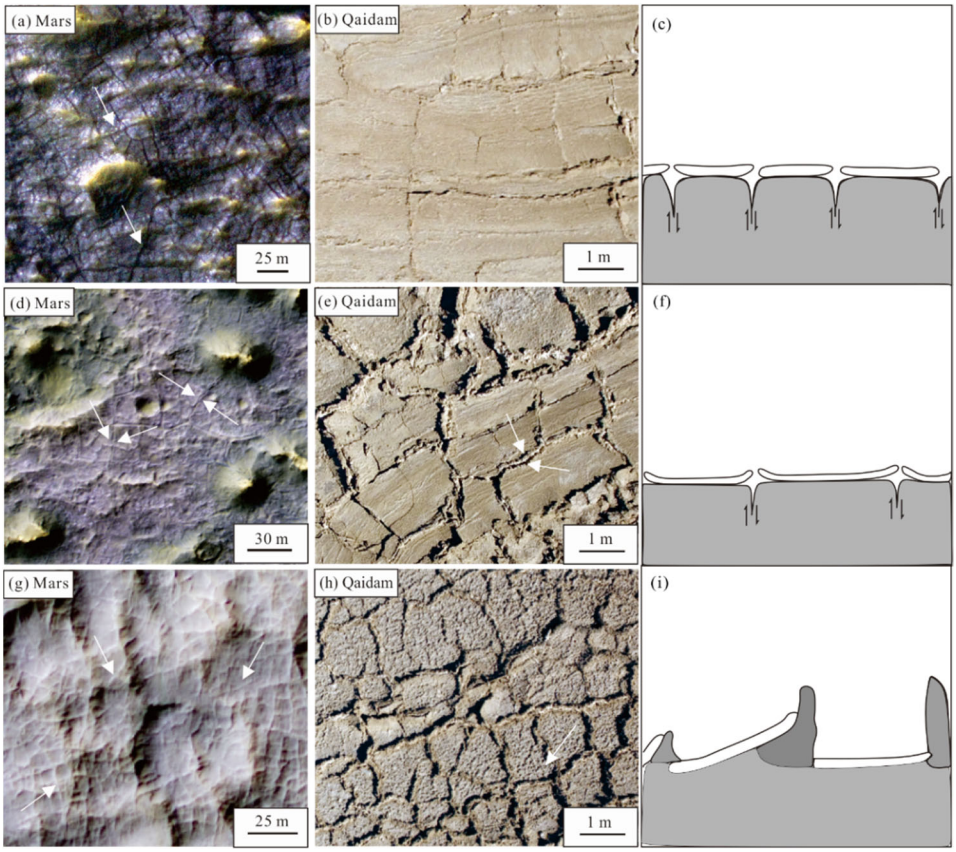

Figure 13. Different stages of salt crust hypothesis for polygonal feature evolution. An example of polygonal fractures of chlorides on Mars (a) and in Qaidam Basin (b 38°2′25″N, 93°8′49″E). A conceptual sketch is illustrated in (c). An example of intermedia polygonal features of chlorides on Mars (d) and in Qaidam Basin (e 38°2′25″N, 93°8′49″E). A conceptual sketch is illustrated in (f). An example of raised ridge polygons of chlorides on Mars (g) and in Qaidam Basin (h 38°2′25″N, 93°8′49″E). A conceptual sketch is illustrated in (i). HiRISE image IDs for (a), (d), (g) are ESP_012575_1470_COLOR, ESP_035866_1610_COLOR, ESP_009846_1475_COLOR, respectively. Images of (b), (e), (h) were collected through a small drone. (c) (f) (i) are modified from (Krinsley, 1970).

3.2 Hydrology Implication of Salt Crust (Raised Ridge Polygonal Features) on Mars

The geologic setting of chlorides is important for us to understand the hydrology about the first billion years of Mars. Lacustrine/playa environment could be a possible geologic setting for the chlorides, which has been proposed by extensive previous studies based on fractures developed in the chlorides and the coexistence with phyllosilicate (El-Maarry et al., 2014, 2013; Ruesch et al., 2012; Glotch et al., 2010; Osterloo et al., 2010, 2008). However, fractures in the chlorides and the presence of phyllosilicate could not well support the playa origin of the chlorides, because there is limited spectral evidence of coexisting of Fe/Mg smectites and chloride (Ruesch et al., 2012; Glotch et al., 2010) and stratigraphy of phyllosilicate with chloride is ambiguous (Huang et al., 2018; El-Maarry et al., 2013; Ruesch et al., 2012; Glotch et al., 2010). Glotch et al. (2010) considered the chlorides deposited later on ancient phyllosilicates basement through groundwater upwelling and alternative exploration suggests the phyllosilicates have the same origin as chlorides, indicating a salt-rich playa setting (El-Maarry et al., 2013). The ambiguous stratigraphy relationship between chloride and phyllosilicate does not fully support the playa geologic setting of the chlorides.

The salt crust is a diagnostic indicator of playa on Earth (Anglés and Li, 2017; Thomas, 2011). We proposed that raised ridge polygonal features we observed experienced similar formation process, and they could serve as the indicator of playa setting on Mars. The salt crust found on chlorides of Mars may indicate multiple groundwater activity after the cease of surface water activity in its early history. Generally, the duration of groundwater activity forming this kind of landform need hundreds of years in terrestrial analogy (Anglés and Li, 2017; Thomas, 2011), which could provide clues to the duration of groundwater activity on early Mars.

3.3 Astrobiology Implication

Playa is a subaqueous habitable environment (Villanueva et al., 2015). The groundwater plays an important role on playa, which can provide a conduit between the subsurface and the surface habitats (Rosen, 1994). The temperature and relative humidity retained by salts in the subsurface layer are tremendously different from the surface condition, which suggests a huge water reservoir on Mars as well as habitability potential (Wang et al., 2018). The chlorides with raised ridge polygonal features are indicators of playa on Mars. In addition, the chlorides are ideal for biosignature preservation, thus they are of great astrobiology interest. Inclusions are common in halite and the fluid inclusions in terrestrial evaporate deposits can provide refuge for extant and

extinct life, preserving biosignatures including DNA, and viable microbial communities over geological timescales, protecting them from hash environment condition, such as highly intense sun light and ultraviolet radiation, rapid changes in salinity and water availability, high salt concentration and desiccation (Stivaletta et al., 2009; Vreeland et al., 2007; Fish et al., 2002). Schubert et al. (2009) have reported resuscitating entrained archea from halite as old as ~34 000 years, and some claims ~10^5 years (Mormile et al., 2003), while another study of Permian halite extended to ~250–300 Ma (Griffith et al., 2008). Retrieval of DNA from these ancient halite samples ranging in age from 11 to 425 Ma were also reported by (Park et al., 2009; Fish et al., 2002; Radax et al., 2001). Therefore, the sites of chlorides with raised ridge polygonal features should be considered as landing sites for future in situ exploration and sample return.

4 CONCLUSION

We used 441 high-resolution orbital images to characterize 153 locations of chlorides with the polygonal features on Mars. We divided these polygonal features into three types based on their geomorphologic characteristics. We ruled out previously proposed hypotheses of the raised ridges polygons in chlorides, and found that the salt crust formation mechanism is most consistent with our observations. Salt crust process is a diagnostic feature of terrestrial playas, which has profound hydrology and astrobiology implication. These chlorides sites with raised ridges polygonal features could indicate playa geologic setting and groundwater activity of early Mars. They are potentially habitable environments, which are of high priority in future missions for biosignature search.

ACKNOWLEDGMENTS

We thank two anonymous reviewers for constructive comments that help to improve the quality of the manuscript. JMARS (https://jmars.asu.edu) and ArcGIS are used in data query, analysis and visualization. All the remote sensing data of Mars are available at the Planetary Data System (https://pds.jpl.nasa.gov). Jun Huang was supported by the National Scientific Foundation of China (Nos. 41403052, 41773061, 41830214), the Fundamental Research Funds for the Central Universities, China University of Geosciences (Wuhan) (Nos. CUGL160402, CUG2017G02) and the Lunar and Planetary Science Laboratory, Macau University of Science and Technology Partner Laboratory of Key Laboratory of Lunar and Deep Space Exploration, Chinese Academy of Sciences (Nos. 039/2013/A2, 121/2017/A3). Binlong Ye was supported by the National Training Program of Innovation and Entrepreneurship for Undergraduates (No. 201610491122). We thank Mr. Jiang Wang and Ms. Ting Huang for their constructive comments of the Qaidam Basin and astrobiology application. The final publication is available at Springer via https://doi.org/10.1007/s12583-019-1212-2.

REFERENCES CITED

Andrews-Hanna, J. C., Lewis, K. W., 2011. Early Mars Hydrology: 2. Hydrological Evolution in the Noachian and Hesperian Epochs. *Journal of Geophysical Research*, 116(E2): E02007. https://doi.org/10.1029/2010je003709

Anglés, A., Li, Y. L., 2017. The Western Qaidam Basin as a Potential Martian Environmental Analogue: An Overview. *Journal of Geophysical Research*: *Planets*, 122(5): 856–888. https://doi.org/10.1002/2017je005293

Bandfield, J. L., 2004. Atmospheric Correction and Surface Spectral Unit Mapping Using Thermal Emission Imaging System Data. *Journal of Geophysical Research*, 109(E10): E10008. https://doi.org/10.1029/2004je002289

Christensen, P. R., Bandfield, J. L., Hamilton, V. E., et al., 2001. Mars Global Surveyor Thermal Emission Spectrometer Experiment: Investigation Description and Surface Science Results. *Journal of Geophysical Research*: *Planets*, 106(E10): 23823–23871. https://doi.org/10.1029/2000je001370

Christensen, P. R., Jakosky, B. M., Kieffer, H. H., et al., 2004. The Thermal Emission Imaging System (THEMIS) for the Mars 2001 Odyssey Mission. *Space Science Reviews*, 110(1/2): 85–130. https://doi.org/10.1023/b:spac.0000021008.16305.94

Christiansen, F. W., 1963. Polygonal Fracture and Fold Systems in the Salt Crust, Great Salt Lake Desert, Utah. *Science*, 139(3555): 607–609. https://doi.org/10.1126/science.139.3555.607

Davila, A. F., Duport, L. G., Melchiorri, R., et al., 2010. Hygroscopic Salts and the Potential for Life on Mars. *Astrobiology*, 10(6): 617–628, https://doi.org/10.1089/ast.2009.0421.

Ebinger, E., Mustard, J., 2015. Linear Ridges in the Nilosyrtis Region of Mars: Implications for Subsurface Fluid Flow. Lunar and Planetary Science Conference, The Woodlands

Edwards, C. S., Christensen, P. R., Hill, J., 2011. Mosaicking of Global Planetary Image Datasets: 2. Modeling of Wind Streak Thicknesses Observed in Thermal Emission Imaging System (THEMIS) Daytime and Nighttime Infrared Data. *Journal of Geophysical Research*, 116(E10): E10005. https://doi.org/10.1029/2011je003857

Ehlmann, B. L., Swayze, G. A., Milliken, R. E., et al., 2016. Discovery of Alunite in Cross Crater, Terra Sirenum, Mars: Evidence for Acidic, Sulfurous Waters. *American Mineralogist*, 101(7): 1527–1542. https://doi.org/10.2138/am-2016-5574

El-Maarry, M. R., Pommerol, A., Thomas, N., 2013. Analysis of Polygonal Cracking Patterns in Chloride-Bearing Terrains on Mars: Indicators of Ancient Playa Settings. *Journal of Geophysical Research*: *Planets*, 118(11): 2263–2278. https://doi.org/10.1002/2013je004463

El-Maarry, M. R., Watters, W., McKeown, N. K., et al., 2014. Potential Desiccation Cracks on Mars: A Synthesis from Modeling, Analogue-Field Studies, and Global Observations. *Icarus*, 241: 248–268. https://doi.org/10.1016/j.icarus.2014.06.033

Fassett, C. I., Head, J. W. III, 2008. Valley Network-Fed, Open-Basin Lakes on Mars: Distribution and Implications for Noachian Surface and Subsurface Hydrology. *Icarus*, 198(1): 37–56. https://doi.org/10.1016/j.icarus.2008.06.016

Fish, S. A., Shepherd, T. J., McGenity, T. J., et al., 2002. Recovery of 16S Ribosomal RNA Gene Fragments from Ancient Halite. *Nature*, 417(6887): 432–436. https://doi.org/10.1038/417432a

Gillespie, A. R., Kahle, A. B., Walker, R. E., 1986. Color Enhancement of Highly Correlated Images. I. Decorrelation and HSI Contrast Stretches. *Remote Sensing of Environment*, 20(3): 209–235. https://doi.org/10.1016/0034-4257(86)90044-1

Glotch, T. D., Bandfield, J. L., Tornabene, L. L., et al., 2010. Distribution and Formation of Chlorides and Phyllosilicates in Terra Sirenum, Mars. *Geophysical Research Letters*, 37(16): 127–137. https://doi.org/10.1029/2010gl044557

Glotch, T. D., Bandfield, J. L., Wolff, M. J., et al., 2016. Constraints on the Composition and Particle Size of Chloride Salt-Bearing Deposits on Mars. *Journal of Geophysical Research*: *Planets*, 121(3): 454–471. https://doi.org/10.1002/2015je004921

Griffith, J. D., Willcox, S., Powers, D. W., et al., 2008. Discovery of Abundant Cellulose Microfibers Encased in 250 Ma Permian Halite: A

Macromolecular Target in the Search for Life on other Planets. *Astrobiology*, 8(2): 215–228. https://doi.org/10.1089/ast.2007.0196

Head, J. W., Mustard, J. F., 2006. Breccia Dikes and Crater-Related Faults in Impact Craters on Mars: Erosion and Exposure on the Floor of a Crater 75 km in Diameter at the Dichotomy Boundary. *Meteoritics & Planetary Science*, 41(10): 1675–1690. https://doi.org/10.1111/j.1945-5100.2006.tb00444.x

Herkenhoff, K. E., Byrne, S., Russell, P. S., et al., 2007. Meter-Scale Morphology of the North Polar Region of Mars. *Science*, 317(5845): 1711–1715. https://doi.org/10.1126/science.1143544

Huang, J., Salvatore, M., Edwards, C., et al., 2018. A Complex Fluviolacustrine Environment on Early Mars and Its Astrobiological Potentials. *Astrobiology*, 18(8): 1081–1091. https://doi.org/10.1089/ast.2017.1757

Hynek, B. M., Beach, M., Hoke, M. R. T., 2010. Updated Global Map of Martian Valley Networks and Implications for Climate and Hydrologic Processes. *Journal of Geophysical Research*, 115(E9): E9008. https://doi.org/10.1029/2009je003548

Hynek, B. M., Osterloo, M. K., Kierein-Young, K. S., 2015. Late-Stage Formation of Martian Chloride Salts through Ponding and Evaporation. *Geology*, 43(9): 787–790. https://doi.org/10.1130/g36895.1

Jensen, H. B., Glotch, T. D., 2011. Investigation of the Near-Infrared Spectral Character of Putative Martian Chloride Deposits. *Journal of Geophysical Research*, 116(E12): E00J03. https://doi.org/10.1029/2011je003887

Kerber, L., Dickson, J. L., Head, J. W., et al., 2017. Polygonal Ridge Networks on Mars: Diversity of Morphologies and the Special Case of the Eastern Medusae Fossae Formation. *Icarus*, 281: 200–219. https://doi.org/10.1016/j.icarus.2016.08.020

Kirk, R. L., Howington-Kraus, E., Rosiek, M. R., et al., 2008. Ultrahigh Resolution Topographic Mapping of Mars with MRO HiRISE Stereo Images: Meter-Scale Slopes of Candidate Phoenix Landing Sites. *Journal of Geophysical Research*, 113(E12): E00A24. https://doi.org/10.1029/2007je003000

Krinsley, D. B., 1970. A Geomorphological and Paleoclimatological Study of the Playas of Iran. *Journal of Hydrology*, 16(1): 66. https://doi.org/10.1016/0022-1694(72)90188-6

Levy, J. S., Head, J. W., Marchant, D. R., 2009b. Concentric Crater Fill in Utopia Planitia: History and Interaction between Glacial "Brain Terrain" and Periglacial Mantle Processes. *Icarus*, 202(2): 462–476. https://doi.org/10.1016/j.icarus.2009.02.018

Levy, J., Head, J., Marchant, D., 2009a. Thermal Contraction Crack Polygons on Mars: Classification, Distribution, and Climate Implications from HiRISE Observations. *Journal of Geophysical Research*, 114(E1): E01007. https://doi.org/10.1029/2008je003273

Malin, M. C., Bell, J. F. III, Cantor, B. A., et al., 2007. Context Camera Investigation on Board the Mars Reconnaissance Orbiter. *Journal of Geophysical Research*, 112(E5): E05S04. https://doi.org/10.1029/2006je002808

Mangold, N., 2005. High Latitude Patterned Grounds on Mars: Classification, Distribution and Climatic Control. *Icarus*, 174(2): 336–359. https://doi.org/10.1016/j.icarus.2004.07.030

Mangold, N., Poulet, F., Mustard, J. F., et al., 2007. Mineralogy of the Nili Fossae Region with OMEGA/Mars Express Data: 2. Aqueous Alteration of the Crust. *Journal of Geophysical Research*: *Planets*, 112(E8): E08S04. https://doi.org/10.1029/2006je002835

McEwen, A. S., Eliason, E. M., Bergstrom, J. W., et al., 2007. Mars Reconnaissance Orbiter's High Resolution Imaging Science Experiment (HiRISE). *Journal of Geophysical Research*, 112(E5): E05S02. https://doi.org/10.1029/2005je002605

Mellon, M. T., Arvidson, R. E., Marlow, J. J., et al., 2008. Periglacial Landforms at the Phoenix Landing Site and the Northern Plains of Mars. *Journal of Geophysical Research*, 113(E4): E00A23. https://doi.org/10.1029/2007je003039

Mellon, M. T., Feldman, W. C., Prettyman, T. H., 2004. The Presence and Stability of Ground Ice in the Southern Hemisphere of Mars. *Icarus*, 169(2): 324–340. https://doi.org/10.1016/j.icarus.2003.10.022

Mellon, M. T., Jakosky, B. M., 1995. The Distribution and Behavior of Martian Ground Ice during Past and Present Epochs. *Journal of Geophysical Research*, 100(E6): 11781–11799. https://doi.org/10.1029/95je01027

Morgenstern, A., Hauber, E., Reiss, D., et al., 2007. Deposition and Degradation of a Volatile-Rich Layer in Utopia Planitia and Implications for Climate History on Mars. *Journal of Geophysical Research*, 112(E6): E06010. https://doi.org/10.1029/2006je002869

Mormile, M. R., Biesen, M. A., Gutierrez, M. C., et al., 2003. Isolation of Halobacterium Salinarum Retrieved Directly from Halite Brine Inclusions. *Environmental Microbiology*, 5(11): 1094–1102. https://doi.org/10.1046/j.1462-2920.2003.00509.x

Murchie, S. L., Mustard, J. F., Ehlmann, B. L., et al., 2009. A Synthesis of Martian Aqueous Mineralogy after 1 Mars Year of Observations from the Mars Reconnaissance Orbiter. *Journal of Geophysical Research*, 114(E2): E00D06. https://doi.org/10.1029/2009je003342

Mutch, T. A., Binder, A. B., Huck, F. O., et al., 1976. The Surface of Mars: The View from the Viking 1 Lander. *Science*, 193(4255): 791–801. https://doi.org/10.1126/science.193.4255.791

Okubo, C. H., McEwen, A. S., 2007. Fracture-Controlled Paleo-Fluid Flow in Candor Chasma, Mars. *Science*, 315(5814): 983–985. https://doi.org/10.1126/science.1136855

Osterloo, M. M., Anderson, F. S., Hamilton, V. E., et al., 2010. Geologic Context of Proposed Chloride-Bearing Materials on Mars. *Journal of Geophysical Research*, 115(E10): E10012. https://doi.org/10.1029/2010je003613

Osterloo, M. M., Hamilton, V. E., Bandfield, J. L., et al., 2008. Chloride-Bearing Materials in the Southern Highlands of Mars. *Science*, 319(5870): 1651–1654. https://doi.org/10.1126/science.1150690

Park, J. S., Vreeland, R. H., Cho, B. C., et al., 2009. Haloarchaeal Diversity in 23, 121 and 419 MYA Salts. *Geobiology*, 7(5): 515–523. https://doi.org/10.1111/j.1472-4669.2009.00218.x

Putzig, N. E., Mellon, M. T., Kretke, K. A., et al., 2005. Global Thermal Inertia and Surface Properties of Mars from the MGS Mapping Mission. *Icarus*, 173(2): 325–341. https://doi.org/10.1016/j.icarus.2004.08.017

Radax, C., Gruber, C., Stan-Lotter, H., 2001. Novel Haloarchaeal 16S RRNA Gene Sequences from Alpine Permo-Triassic Rock Salt. *Extremophiles*, 5(4): 221–228. https://doi.org/10.1007/s007920100192

Rosen, M. R., 1994. The Importance of Groundwater in Playas: A Review of Playa Classification and the Sedimentology and Hydrology of Playas, GSA Special Papers 289, Geological Society of America, Boulder, Co.

Ruesch, O., Poulet, F., Vincendon, M., et al., 2012. Compositional Investigation of the Proposed Chloride-Bearing Materials on Mars Using Near-Infrared Orbital Data from OMEGA/MEx. *Journal of Geophysical Research*: *Planets*, 117(E11): E00J13. https://doi.org/10.1029/2012je004108

Saper, L., Mustard, J. F., 2013. Extensive Linear Ridge Networks in Nili Fossae and Nilosyrtis, Mars: Implications for Fluid Flow in the Ancient Crust. *Geophysical Research Letters*, 40(2): 245–249. https://doi.org/10.1002/grl.50106

Schubert, B. A., Lowenstein, T. K., Timofeeff, M. N., 2009. Microscopic Identification of Prokaryotes in Modern and Ancient Halite, Saline Valley and Death Valley, California. *Astrobiology*, 9(5): 467–482. https://doi.org/10.1089/ast.2008.0282

Shean, D. E., Alexandrov, O., Moratto, Z. M., et al., 2016. An Automated, Open-Source Pipeline for Mass Production of Digital Elevation Models (DEMs) from Very-High-Resolution Commercial Stereo Satellite

Imagery. *ISPRS Journal of Photogrammetry and Remote Sensing*, 116: 101–117. https://doi.org/10.1016/j.isprsjprs.2016.03.012

Soare, R. J., Osinski, G. R., Roehm, C. L., 2008. Thermokarst Lakes and Ponds on Mars in the very Recent (Late Amazonian) Past. *Earth and Planetary Science Letters*, 272(1/2): 382–393. https://doi.org/10.1016/j.epsl.2008.05.010

Stein, N., Grotzinger, J. P., Schieber, J., et al., 2018. Desiccation Cracks Provide Evidence of Lake Drying on Mars, Sutton Island Member, Murray Formation, Gale Crater: REPLY. *Geology*, 46(8): e450–e450. https://doi.org/10.1130/g45237y.1

Stivaletta, N., Barbieri, R., Picard, C., et al., 2009. Astrobiological Significance of the Sabkha Life and Environments of Southern Tunisia. *Planetary and Space Science*, 57(5/6): 597–605. https://doi.org/10.1016/j.pss.2008.10.002

Thomas, D. S. G., 2011. Arid Zone Geomorphology: Process, Form and Change in Drylands. Wiley

Villanueva, G. L., Mumma, M. J., Novak, R. E., et al., 2015. Strong Water Isotopic Anomalies in the Martian Atmosphere: Probing Current and Ancient Reservoirs. *Science*, 348(6231): 218–221. https://doi.org/10.1126/science.aaa3630

Vreeland, R. H., Jones, J., Monson, A., et al., 2007. Isolation of Live Cretaceous (121–112 Million Years Old) Halophilic Archaea from Primary Salt Crystals. *Geomicrobiology Journal*, 24(3/4): 275–282. https://doi.org/10.1080/01490450701456917

Wang, A. L., Sobron, P., Kong, F., et al., 2018. Dalangtan Saline Playa in a Hyperarid Region on Tibet Plateau: II. Preservation of Salts with High Hydration Degrees in Subsurface. *Astrobiology*, 18(10): 1254–1276. https://doi.org/10.1089/ast.2018.1829

Wang, C. W., Hong, H. L., Li, Z. H., et al., 2013. Climatic and Tectonic Evolution in the North Qaidam since the Cenozoic: Evidence from Sedimentology and Mineralogy. *Journal of Earth Science*, 24(3): 314–327. https://doi.org/10.1007/s12583-013-0332-3

Wray, J. J., Milliken, R. E., Dundas, C. M., et al., 2011. Columbus Crater and other Possible Groundwater-Fed Paleolakes of Terra Sirenum, Mars. *Journal of Geophysical Research*, 116(E1): E01001. https://doi.org/10.1029/2010je003694

Wray, J. J., Murchie, S. L., Squyres, S. W., et al., 2009. Diverse Aqueous Environments on Ancient Mars Revealed in the Southern Highlands. *Geology*, 37(11): 1043–1046. https://doi.org/10.1130/g30331a.1

Xiao, L., Wang, J., Dang, Y. N., et al., 2017. A New Terrestrial Analogue Site for Mars Research: The Qaidam Basin, Tibetan Plateau (NW China). *Earth-Science Reviews*, 164: 84–101. https://doi.org/10.1016/j.earscirev.2016.11.003

Yi, L. W., Gu, X. P., Lu, A. H., et al., 2017. Atacamite and Nantokite in Kaerqueka Copper Deposit of Qimantag Area: Evidence for Cenozoic Climate Evolution of the Qaidam Basin. *Journal of Earth Science*, 28(3): 492–499. https://doi.org/10.1007/s12583-017-0548-8

Zanetti, M., Hiesinger, H., Reiss, D., et al., 2010. Distribution and Evolution of Scalloped Terrain in the Southern Hemisphere, Mars. *Icarus*, 206(2): 691–706. https://doi.org/10.1016/j.icarus.2009.09.010

Zeng, F. M., Xiang, S. Y., 2017. Geochronology and Mineral Composition of the Pleistocene Sediments in Xitaijinair Salt Lake Region, Qaidam Basin: Preliminary Results. *Journal of Earth Science*, 28(4): 622–627. https://doi.org/10.1007/s12583-016-0712-6